of 10, 25 and 50 kGy were respectively 195,000, 142,000 and 95,000 by GPC.

Micromass Culture of Osteoblasts. Mouse osteoblast-like MC3T3-E1 cells (RIKEN Cell Bank, Japan) and normal human osteoblast NHOst cells (Clonetics Corporation, MD, USA) were grown in alpha minimum essential medium (α-MEM) supplemented with 20% fetal bovine serum. The PLLA sheet was cut into 14.0 mm diameter disk and laid in a 24-well dish. The 20 μl of cell suspension (2×10^6 cells/ml) was delivered on the disk. After the cells were attached on the disk, 1 ml of the complete medium that contained 10 mM disodium β-glycerophosphate in the culture medium was added. The complete medium was changed three times a week, and the cells cultured for 2 weeks in a 37°C humidified atmosphere of 5% CO_2.

Proliferation Assay. The number of the cells cultured on the PLLA sheet was determined by WST-8 assay [5]. Moreover, the protein and DNA contents of the cell lysate were measured by the Lowry method and the fluorescence assay using Hoechst 33258 dye, respectively [5].

Differentiation Assay. The calcium depositions of the cell cultures were stained by alizarin red S, and the areas stained dark-red were measured using the program Scion Image (Scion Co., MD, USA) [5]. The calcification was calculated as the normalized area in the cell number. Moreover, the collagen synthesis was evaluated by the hydroxyproline content of the cell lysate, and ALP activity of the cells was measured using *p*-nitrophenylphosphate as a substrate [5].

Soaking in the Medium. The PLLA sheet was cut into 14.0 mm diameter disk and laid in a 24-well dish. The complete medium of 1 ml was added without the cells. Then, the dish was stored in a 37°C humidified atmosphere of 5% CO_2, and the complete medium was changed three times a week. After soaking for 2 weeks, the PLLA disk was washed in deionized water five times quickly and dried in a silica gel desiccator.

Surface Analysis. The surface of the PLLA sheet after soaking in the complete medium without the cells was characterized by SEM, EDX, FT-IR and XPS according to the conventional methods.

Results

Proliferation of Osteoblasts Cultured on the PLLA Sheet. The cell number of MC3T3-E1 cells cultured on the PLLA sheet did not change with increasing irradiation dose (Fig. 1a). The protein and DNA contents of the cells also did not change. The other side, the cell number (Fig. 1b),

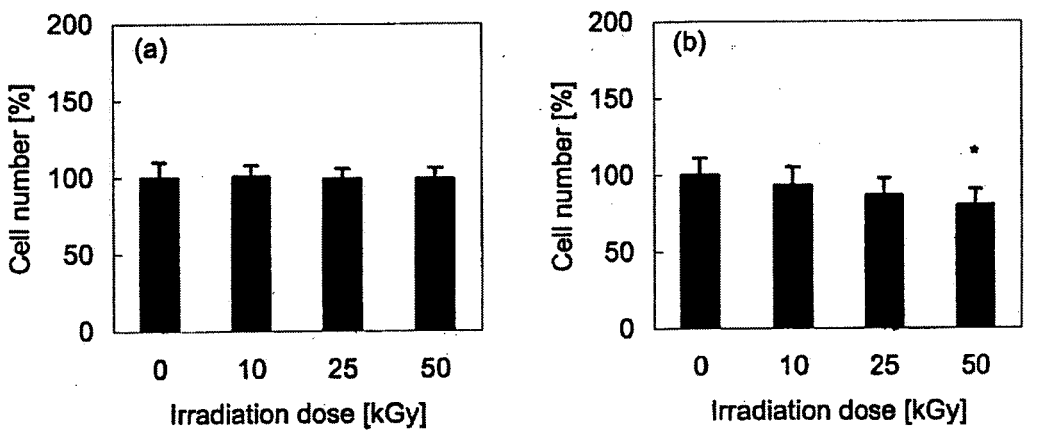

Fig. 1. The cell numbers of (a) MC3T3-E1 and (b) NHOst cells cultured on the γ-irradiated PLLA sheet.

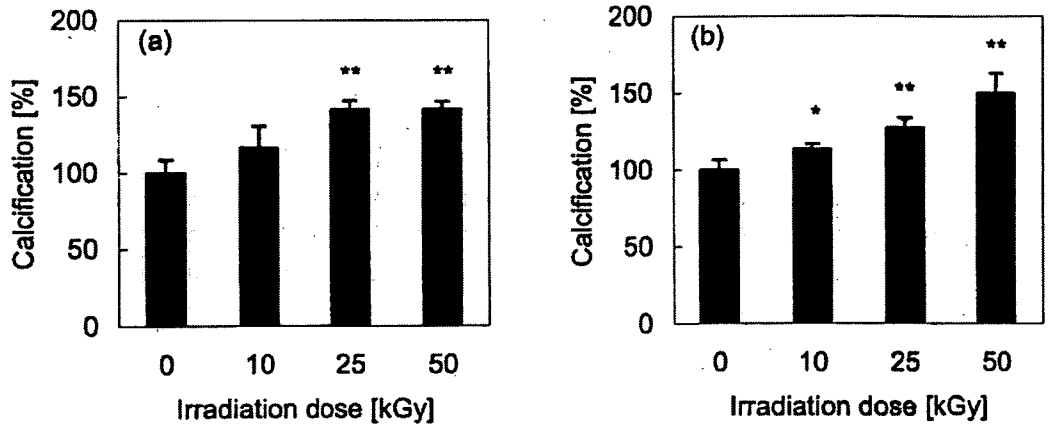

Fig. 2. The calcifications of (a) MC3T3-E1 and (b) NHOst cells cultured on the γ-irradiated PLLA sheet.

protein and DNA contents of NHOst cells cultured on the PLLA sheet slightly decreased with irradiation dose.

Differentiation of Osteoblasts Cultured on the PLLA Sheet. The calcification of MC3T3-E1 cells (Fig. 2a) and NHOst cells (Fig. 2b) remarkably increased with irradiation dose. The collagen synthesis and ALP activity of MC3T3-E1 and NHOst cells also increased as same as the calcification, respectively. The γ-irradiated PLLA remarkably promoted the differentiation of osteoblasts.

Apatite Formation on the PLLA Sheet. The SEM micrograph exhibited crystal particles on the surface of the PLLA sheet after soaking in the complete medium without the cells. The crystal particles were identified with hydroxyapatite by EDX, FT-IR and XPS spectra. The phosphate band in ATR/FT-IR spectra became strong with irradiation dose (Fig. 3). Moreover, the element rations of calcium and phosphorus increased but that of carbon decreased with irradiation dose, in XPS analysis (Fig. 4). The amount of hydroxyapatite formed on the γ-irradiated PLLA sheet increased with irradiation dose.

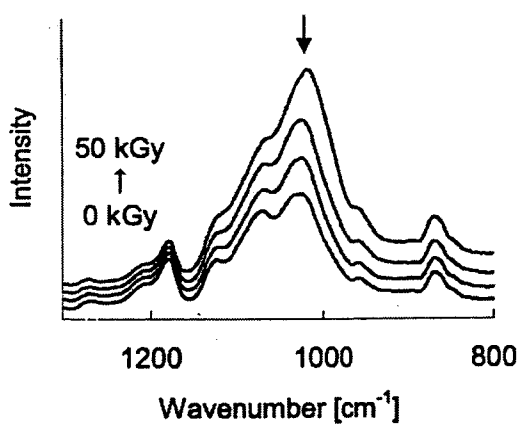

Fig. 3. The phosphate band of the γ-irradiated PLLA sheet after soaking in the medium.

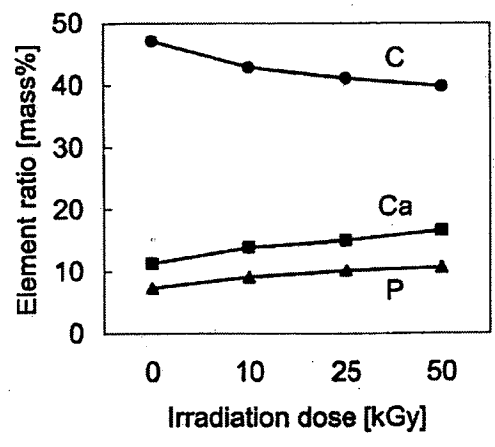

Fig. 4. The element ratios of calcium, phosphorus and carbon of the γ-irradiated PLLA sheet after soaking in the medium.

Discussion

In the present study, the γ-irradiated PLLA hardly affected the proliferation but remarkably promoted the differentiation of osteoblasts. It was expected that the low molecular weight PLLA eluted to the medium, because the molecular weight of PLLA decreased by γ-irradiation. In our recent studies, the low molecular weight PLLA enhanced the differentiation of MC3T3-E1 cells but inhibited that of NHOst cells [6, 7]. The present results, which the differentiations of MC3T3-E1 and NHOst cells both increased on the γ-irradiated PLLA sheet, would not be caused by the low molecular weight PLLA. The surface of the γ-irradiated PLLA should good influence on the differentiation of osteoblasts.

On the other hand, the γ-irradiation increased the apatite-forming ability of the PLLA sheet. Tanahashi and Matsuda reported that some negatively charged groups such as phosphate and carboxyl group strongly induced apatite formation in a simulated body fluid. They described that the apatite formation was initiated via calcium ion-absorption upon complexation with a negative surface-charged group [8]. In our study, the molecular weight of PLLA decreased with hydrolysis of ester bonds by γ-irradiation [2]. Therefore, the amount of carboxyl group of the γ-irradiated PLLA would increase with irradiation dose, and the carboxyl group would promote the apatite-forming ability of the PLLA sheet.

Fujibayashi *et al.* compared *in vivo* bone ingrowth and *in vitro* apatite formation on Na_2O-CaO-SiO_2 glasses. The quantities of newly bone formed on the glasses correlated with their apatite-forming abilities in simulated body fluid. They propose to evaluate the apatite-forming ability in order to confirm the *in vivo* bioactibity of biomaterials [9]. In our present study, the γ-irradiation enhanced the apatite-forming ability of the PLLA sheet, and then the γ-irradiated PLLA sheet promoted the differentiation of osteoblasts. The osteoblast differentiation should connect with the apatite formation on the γ-irradiated PLLA sheet.

In conclusion, the γ-irradiated PLLA hardly affected the proliferation but promoted the differentiation of osteoblasts with increasing irradiation dose. On the other hand, the hydroxyapatite was formed on the PLLA sheet in the medium, and the γ-irradiation enhanced apatite-forming ability of the PLLA. It was suggested that the connection between the osteoblast differentiation and apatite formation on the γ-irradiated PLLA sheets.

References

[1] T.E. Otto, P. Patka, H.J.Th.M. Haarman, C.P.A.T. Klein and R. Vriesde: J. Mater. Sci. Mater. Med. 5 (1994), 407-410.

[2] K. Isama and T. Tsuchiya: Bull. Natl. Inst. Health Sci. 119 (2001), 61-64.

[3] X. Yuan, A.F.T. Mak and J. Li: J. Biomed. Mater. Res. 57 (2001), 140-150.

[4] N. Olmo, A.I. Martin, A.J. Salinas, J. Turnay, M. Vallet-Regi and M.A. Lizarbe: Biomaterials 24 (2003), 3383-3393.

[5] K. Isama and T. Tsuchiya: J. Biomater. Sci. Polymer Edn. 13 (2002), 153-166.

[6] K. Isama and T. Tsuchiya: Biomaterials 24 (2003), 3303-3309.

[7] K. Isama, Y. Ikarashi and T. Tsuchiya: BIO INDUSTRY 19 (2002), 21-29.

[8] M. Tanahashi and T. Matsuda: J. Biomed. Mater. Res. 34 (1997), 305-315.

[9] S. Fujibayashi, M. Neo, H.M. Kim, T. Kokubo and T. Nakamura: Biomaterials 24 (2003), 1349-1356.

再生医療・繊維工学・人工臓器に使用される医療用材料の安全性・有効性に関する基本的考え方

Standpoints and Principles for the Evaluation of Safety and Efficacy of Biomaterials Applied for Tissue Engineered Products

土屋利江

1. はじめに

国内外共に開発競争が盛んな医療材料の一つとして生分解性材料があげられる。限られた紙面の都合上、ここでは、注目されている生分解性材料において、現在、安全性・有効性において問題になっている点を中心に述べる。生分解性材料は、やがては生体内で消失し、残存しないという長所があるものの、吸収性材料であるが故に、クラスⅣに分類されるハイリスク医療材料である。最近の不具合報告や前臨床試験研究からも、解決すべきいくつかのポイントがあるので、現在考えられる基本的考え方について述べる。

2. 安全性

各種モノマーから合成される高分子系では、使用される触媒の選択が安全性・有効性を考える上で第1のキーポイントとなる。環境および生体ハザードとして有名な触媒を使用している例がある。生分解性材料を医療材料として使用した場合、生体内で吸収される。使用される材料のトータル量は医療材料の使用目的によって数mgから数g程度まで異なっている。量が多くなると安全性上のリスクも高くなる。安全性上問題はないのか最新の知見を十分検討して合成のスキームを描いていただきたい。また、医療材料として使用する場合、使用する部位、使用する量、分解速度によって安全性に関するリスクレベルは異なる。慎重な検討を御願いしたい。

3. 経済性と安全性

医療材料も、エコマテリアルであることが、理想的であるが、通常、工業製品用のエコマテリアルとなると数百から数千トン単位で合成され、地球環境系へ放出される。また、使用量も多く、できるだけ低コストで生産されることになる。工業界では、安価な触媒で効率よく重合できる製法が望まれる。安全性に対する検討事項もあるが、医療材料として使用される場合とは試験選択項目が異なる。分解性という点でエコマテリアルの候補と考えられるポリグリコール酸には、環境ハザードで有名な有機錫で合成された製品が販売されている例がある。有機錫は、ppbあるいはそれ以下のオーダーで神経毒性を示す触媒である。作用域が低濃度であるため、残留物の分析では、一般化学分析では、同定・定量することは容易ではない。製造工程が示してあれば、容易に知ることが可能であるが、カタログ掲載の製品では、使用されている触媒が、明示されていないし、たづねても回答がかえってこないケースが多い。世の中に登場しているエコマテリアルと称される材料が、安全性上、危惧される点が解決できた製造工程で合成されているか確認する必要がある。環境中に放出されれば、触媒は、土壌中に残留することになり、海にも流れ、やがては、魚貝類に蓄積し、食物連鎖によりやがてはヒトの健康への悪影響が懸念される。これらの点は、逆の発想をすれば、有効性の高い材料開発のアイデアともなりうる。すなわち、毒性のある触媒の代わりに、有効性の高い触媒を使用すれば、安全で有効性の高い材料開発の創製となるかもしれない。

海外では、すでに無触媒条件下で分子量100万のレベルまで重合した生分解製材料を高価な価格で販売しているという。この分野の国際情報の流通がわるい。

4. 生体適合性

第2のポイントは、生体内に埋植すると炎症反応を惹起しやすい性質を示す材料がある。炎症反応が起これば、例えば、バイオ軟骨において、動物に細胞組み込み型生分解性スキャホールドを埋植し、炎症がおきれば、スキャホールドに播種した軟骨細胞等の分化発現や機能維持の目的を達成できない。従って、このような材料に起因した炎症反応を回避あるいは消失させるための創意工夫をしていただきたい。炎症反応惹起の有無はin vivoで確認する必要がある。ある生分解性高分子がらなる材料に軟骨細胞を播種してin vitro培養すると分化を非常によく促進する。次に、動物の軟骨欠損部分に移植したところ、組織再生がうまくいかない、材料や細胞組み込み型材料を埋植すると組織再生は遅延し、それらをまったく埋植しない軟骨欠損のまま

TOSHIE TSUCHIYA
国立医薬品食品衛生研究所　療品部長
〒158-8501　東京都世田谷区上用賀1-18-1
Tel：03-3700-9196　Fax：03-3700-9196
E-mail：tsuchiya@nihs.go.jp
〈専門〉繊維工学、医療材料の安全性と生体適合性

の群の自然治癒率がもっとも優れていたということも実際ありうる。Tissue Engineering関連の論文で掲載されたデータで、in vitroでどんなに成績が良くても、生体内で、同じように作用するか否かは、別の問題となる。in vitroで優れた成績を示している必要性はあるが、必ずしもin vivoで成功するとは限らない。生体内は、複数の細胞・組織のネットワークで営まれております。in vitro系は、特定の細胞の反応をみていること、さらに、検出している指標のみを解析しているにすぎないことを、いつも考慮しておく必要がある。

5. 更なる生体適合性

第3のポイントは、合成高分子には、ゲッシ類で比較的高い腫瘍発生率を示す材料があることに留意して、新たな材料開発を行うべきである。たとえば、京都大学の研究成果では、ポリグリコール酸は、フィルムをラット皮下に長期間埋植しても、腫瘍の発生を認めなかったが、ポリ乳酸フィルムを、ラット皮下に埋植した結果、埋植ラットの40%に腫瘍発生を認めている。ポリカプロラクトンとの共重合体では、50%の腫瘍発生頻度であった。一方、材料発癌では、20年以上昔の現象から、フィルム状のものをゲッシ類の皮下に埋植すると、腫瘍を発生する。との古典的な説がある。フィルムがすべて同程度腫瘍化するわけではない。シリコンフィルムでは、手術群に近く、低発生率である。フィルムで腫瘍発生する生分解性材料を、粒子状にして埋植した結果、やはり腫瘍を発生し、発生率は、埋植量に比例した。私は、埋植材料の化学組成、物理学的性質、残留性(分解速度)、血管系の有無などがサイトカイン産生、コネキシン機能変化、炎症反応による活性酸素産生、修復能などに影響を与え、腫瘍発生率に関係すると考えている。

医療材料の安全性評価においては、ガイドラインにある一通りの試験項目について受託機関等により試験し、すべて陰性結果を得ると、安全であると考えやすいが、その試験が適切な抽出やサンプル適用方法でおこなわれていない限り、意味のない試験結果となることを強調しておく。生分解性材料の場合に、そのオリゴマーの安全性についても評価することが、長期予測をおこなう上で重要である。

第10回高分子分析討論会(高分子の分析及びキャラクタリゼーション)－研究発表募集－

主　催：日本分析化学会高分子分析研究懇談会　　**協　賛**：㈳繊維学会　　**日　時**：平成17年10月27日(木)・28日(金)
会　場：工学院大学新宿校舎〔東京都新宿区西新宿1-24-2、交通：JR(山手線・中央線・埼京線)、京王線、小田急線、地下鉄(丸の内線・都営新宿線)「新宿」駅下車西口より徒歩5分。大江戸線「都庁前」駅直結〕
http://www.kogakuin.ac.jp/mnp/shinjuku/map_shinjuku.pdf
発表申込締切：7月1日(金)　　**発表要旨締切**：10月7日(金)
研究発表申込先・問合先：〒305-8565　茨城県つくば市東1-1-1　つくば中央5
(独)産業技術総合研究所　計測標準研究部門　有機分析科　高分子標準研究室　松山重倫
TEL：029-861-4617、FAX：029-861-4618、E-mail：polymer@m.aist.go.jp

---

第41回X線分析討論会－講演募集－

主　催：日本分析化学会X線分析研究懇談会　　**協　賛**：㈳繊維学会ほか
日　時：平成17年10月21日(金)・22日(土)
会　場：京都大学福井謙一記念研究センター(京都市左京区高野西開町34-4)
講演申込締切日：8月10日(水)　　**講演要旨締切日**：9月16日(金)
詳細については下記にお問い合せください。
〒141-0031　品川区西五反田1-26-2　五反田サンハイツ304号　日本分析化学会X線分析研究懇談会
TEL：03-3490-3351　FAX：03-3490-3572　E-mail：ktanaka@jsac.or.jp

「高分子材料の耐久性評価」に関する講習会

主　催：日本材料学会　　**協　賛**：㈳繊維学会ほか　　**日　時**：平成17年7月22日(金)　9：30～14：40
会　場：工学院大学新宿校舎28階第1会議室　〒163-8677　東京都新宿区西新宿1-24-2(TEL：03-3342-1211)
プログラム、参加申込の詳細については、下記にお問い合せください。
〒606-8301　京都市左京区吉田泉殿町1-101　日本材料学会「高分子材料の耐久性評価」講習会係
TEL：075-761-5321　FAX：075-761-5325　E-mail：jimu@jsms.jp

STEM CELLS®
Tissue-Specific Stem Cells

Limbal Epithelial Side-Population Cells Have Stem Cell–Like Properties, Including Quiescent State

TERUMASA UMEMOTO,[a] MASAYUKI YAMATO,[a] KOHJI NISHIDA,[b] JOSEPH YANG,[a] YASUO TANO,[b] TERUO OKANO[a]

[a]Institute of Advanced Biomedical Engineering and Science, Tokyo Women's Medical University, Tokyo, Japan; [b]Department of Ophthalmology, Osaka University Medical School, Osaka, Japan

Key Words. Side population • Quiescence • ABCG2 • Limbal epithelium • Corneal epithelium

ABSTRACT

Corneal epithelial (CE) stem cells are believed to reside in the basal layer of the limbal epithelium but remain poorly understood due to the lack of an accepted in vivo reconstitution assay as well as definitive markers for epithelial stem cells. It has been reported that side-population (SP) cells with the ability to efflux the DNA-binding dye Hoechst 33342 have stem cell–like properties and that the SP phenotype accurately represents a quiescent and immature stem cell population in the adult bone marrow. In the present study, we investigated whether SP cells isolated from the limbal epithelium have stem cell–like properties. SP cells, separated by fluorescence-activated cell sorting, comprise approximately 0.4% of all limbal epithelial cells and have markedly higher expression of the stem cell markers ABCG2, Bmi-1, and nestin but no expression of markers for differentiated CE cells compared with non-SP cells. Cell-cycle and telomerase activity analyses revealed that SP cells are growth arrested and reside in the quiescent state. Moreover, limbal epithelial SP cells did not demonstrate proliferative capabilities under typical in vitro epithelial cell culture conditions using 3T3 feeder layers. These findings present the possibility that quiescent limbal epithelial SP cells may represent an extremely immature stem cell population compared with currently defined epithelial stem or progenitor cells. STEM CELLS *2006;24:86–94*

INTRODUCTION

Adult tissue-specific stem cells have the unique ability for self-renewal and govern the maintenance of their tissue of origin. These stem cells, which reside in specialized niches, are vital in sustaining long-term repopulation of the specific tissue via progression through a series of increasingly differentiated cells. Adult stem cells are particularly resistant to various stresses, and the proper regulation of the stem cell niche is required in maintaining their immature, undifferentiated form. Of all adult lineages, hematopoietic stem cells (HSCs) are the most well-established, as there is significant knowledge and insight into the factors and characteristics that are necessary for the regulation of their self-renewal and differentiation. HSCs previously have been shown to be both quiescent and antiapoptotic, meeting the criteria for tissue-specific adult stem cells [1]. This noncycling state is believed to protect HSCs from external stresses and allows for the maintenance of their self-renewal. It has recently been demonstrated that the single characteristic that

Correspondence: Professor Teruo Okano, Ph.D., Institute of Advanced Biomedical Engineering and Science, Tokyo Women's Medical University, 8-1 Kawada-cho, Shinjuku-ku, Tokyo 162-8666, Japan. Telephone: 81-3-3353-8111, ext. 30233; Fax: 81-3-3359-6046; e-mail: tokano@abmes.twmu.ac.jp Received February 17, 2005; accepted for publication July 1, 2005; available online without subscription through the open access option. 1066-5099/2006/$12.00/0 doi: 10.1634/stemcells.2005-0064

most accurately represents quiescent HSCs is the side-population (SP) phenotype [1, 2]. SP cells have the unique ability to efflux the DNA-binding dye Hoechst 33342 via the ATP-binding cassette transporter G2 (ABCG2), a member of the multiple-drug resistance family of membrane transporters [3–6]. Bone marrow SP cells have the capability for the long-term multilineage reconstitution of the hematopoietic system [2, 7], and it is believed that these SP cells represent quiescent HSCs more accurately than HSCs characterized by other means. In addition, SP cells have been isolated from various other adult tissues, including liver [8, 9], skeletal muscle [10], and lung [11], demonstrating that this phenotype with the existence of ABCG2 and the ability to efflux Hoechst 33342 may represent a common feature of all adult stem cells.

Corneal epithelial (CE) stem cells are thought to reside in the basal layer of the limbus [12, 13], the transitional zone between the cornea and the peripheral bulbar conjunctiva. CE stem cells maintain the ocular surface by generating transient amplifying (TA) cells that migrate, proliferate, and differentiate to replace lost or damaged CE cells [14–16]. Whereas traditional methods use colony-forming assays or pulse-chase experiments of labeled thymidine, the lack of both definitive markers and an established in vivo reconstitution assay still remain serious obstacles in the unequivocal identification of not only CE stem cells but also other epithelial stem cells. Recently we have demonstrated that the limbal epithelium contains SP cells that express ABCG2 [17]. It is believed that these cells may allow for the separation of CE stem cells from their more differentiated progeny. We therefore investigated the properties of limbal epithelial SP cells to determine whether they possess stem cell–like properties. Our results demonstrate that limbal epithelial SP cells closely resemble HSCs and strongly suggest that these cells allow for the first insights into a true epithelial stem cell population.

Materials and Methods

Cell Preparation

Corneoscleral rims were obtained from New Zealand white rabbits. Limbal tissues were obtained with scissors, and 2.0-mm-diameter portions of the central corneas were obtained by trephination. Excised tissues from the limbus and central corneas were treated with Dulbecco's modified Eagle's medium (DMEM) containing 250 U/ml dispase II (Godo Shusei, Tokyo, Japan, http://www.godo.jp) at 37°C for 1 hour. Epithelial cells were then separated under a dissecting microscope and treated with 0.25% trypsin/1 mM EDTA solution (Invitrogen, Carlsbad, CA, http://www.invitrogen.com) for 20 minutes at 37°C to create single-cell suspensions from the limbal epithelium and corneal epithelium, and enzymatic activity was stopped by adding an equal volume of DMEM containing 10% fetal bovine serum (FBS) (Moregate BioTech, Queensland, Australia, http://www.moregatebiotech.com).

Hoechst 33342 Exclusion Assay Using Fluorescence-Activated Cell Sorting

Limbal epithelial and CE cells were resuspended at a concentration of 10^6 cells/ml in staining medium (DMEM containing 2% FBS and 10 mM HEPES). Cell suspensions were incubated in staining medium containing 3 μg/ml Hoechst 33342 (Sigma, St. Louis, http://www.sigmaaldrich.com) for 90 minutes at 37°C. For inhibition experiments, 50 μM of either R(+)-verapamil (Sigma) or tryprostatin-A (Alexis Biochemicals, Carlsbad, CA, http://www.alexis-corp.com) was added to the staining medium 30 minutes before the addition of Hoechst 33342. After staining, cells were washed two times with Dulbecco's phosphate-buffered saline (PBS) containing 2% FBS and 1 mM HEPES and then resuspended. Before analysis and cell sorting, propidium iodide (Sigma) was added at a final concentration of 2 μg/ml to distinguish between live and nonviable cells. Analysis and cell sorting were performed using a dual-laser fluorescence-activated cell sorter (FACS) (EPICS® ALTRA FACS analysis system, Beckman Coulter, Fullerton, CA, http://www.beckmancoulter.com). Hoechst 33342 was excited at 350 nm using a UV laser, and fluorescence emission was detected through 450-nm band-pass (BP) (Hoechst blue) and 675-nm long-pass (Hoechst red) filters, respectively. Propidium iodide was excited at 488 nm (argon ion laser), and fluorescence emission was detected through a 610-nm BP filter.

Gene Expression Analysis

After sorting and isolation of SP and non-SP (NSP) cells from the limbal epithelium and viable CE cells from central corneas, total RNA was obtained from 10,000 SP, NSP, and CE cells using ISOGEN (Nippon Gene, Tokyo, Japan, http://www.nippongene.com) according to the manufacturer's suggested protocol. After treatment with DNase I (Nippon Gene), single-stranded cDNA was created with the Superscript First-Strand System for reverse transcription–polymerase chain reaction (RT-PCR) (Invitrogen) and used as PCR templates. Primer pairs and TaqMan MGB probes labeled with 6-carboxyfluorescein (FAM) at the 5′-end and nonfluorescent quencher at the 3′-end were designed with Assay-by-Design (Applied Biosystems, Foster City, CA, http://www.appliedbiosystems.com). Quantitative PCR was performed with an iCycler iQTM Real-Time Detection System (Bio-Rad, Hercules, CA, http://www.bio-rad.com). Thermocycling programs consisted of an initial cycle at 50°C for 2 minutes and 95°C for 10 minutes, followed by 50 cycles of 95°C for 15 seconds and 60°C for 1 minute. Negative con-

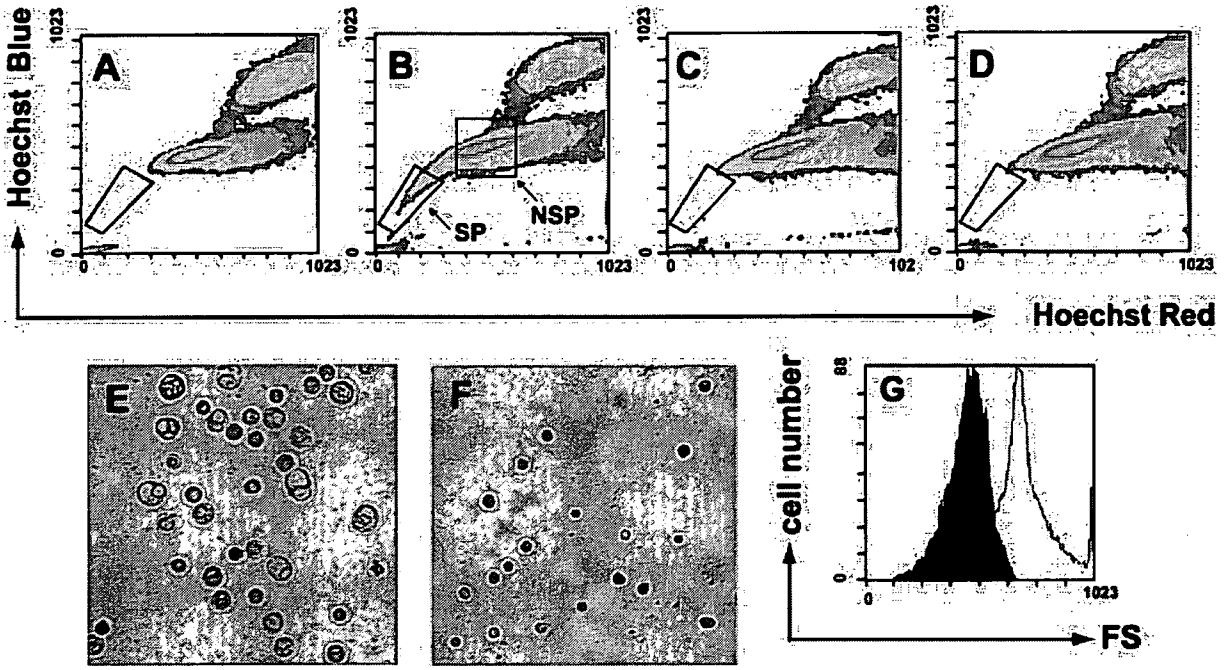

Figure 1. Hoechst 33342 staining in rabbit limbal and corneal epithelial cells. Epithelial cells were removed from the limbus and cornea and analyzed for Hoechst 33342 efflux by fluorescence-activated cell sorting (FACS). Side-population (SP) cells were detected in epithelial cells after Hoechst 33342 staining from the cornea (**A**) and the limbus (**B**). In the density plot of (**B**), the cells denoted by each enclosed area were regarded as SP cells or non-SP (NSP) cells for further characterization. Limbal epithelial cells were pretreated with each transporter inhibitor, verapamil, an inhibitor of MDR (**C**), or tryprostatin-A (TPS-A), a specific inhibitor of ABCG2 (**D**), before staining with Hoechst 33342. After isolation, NSP cells (**E**) and SP cells (**F**) were centrifuged onto glass slide slips and observed with a phase-contrast microscope (magnification ×100). Forward scatter (FS) by FACS was analyzed in SP (black) and NSP (white) cells to examine cell size in each fraction (**G**).

trols using non–reverse transcribed total RNA as template strands were performed for all experiments. All assays were run in duplicate for more than four individual samples. mRNA expression levels were normalized with the expression level of glyceraldehyde-3-phosphate dehydrogenase (GAPDH). To represent expression levels of individual mRNAs, we used an mRNA expression index that divided the value of the specific gene copies by the value for GAPDH. To compare mRNA expression between SP and NSP cells, the Mann-Whitney rank-sum test was applied and statistics were calculated using SigmaStat 2.0 (SPSS, Chicago, IL, http://www.spss.com).

Colony-Forming Assay

Feeder layers were prepared by seeding of mitomycin C–treated NIH-3T3 cells at a density of 2 × 104 cells/cm^2, and SP, NSP, or all viable limbal epithelial cells were seeded at a density of 1,000 cells per 60-mm dish (Becton, Dickinson and Company, Franklin Lakes, NJ, http://www.bd.com). After culture for approximately 10 days at 37°C, colonies were fixed with 10% formalin (Wako Chemicals, Osaka, Japan, http://www.wako-chem.co.jp/english) and stained with 2% rhodamine B (Sigma), and the entire dish surfaces were scanned under a dissecting microscope.

Cell-Cycle Analysis

Limbal epithelial SP cells and total limbal epithelial cells were pelleted by centrifugation and resuspended in a solution containing 4 mM sodium citrate (pH 7.6), 0.2% Nonidet P-40, and 50 μg/ml propidium iodide. After incubation on ice for 30 minutes, cell suspensions were treated with 0.25 mg/ml RNase A for 15 minutes at 37°C to remove double-stranded RNA. Cells were finally analyzed by flow cytometry at an excitation wavelength of 488 nm.

Telomerase Activity

Using the TRAPeze XL telomerase Detection Kit (Chemicon, Temecula, CA, http://www.chemicon.com), telomerase activity was investigated in SP, NSP, and corneal epithelial cells according to the manufacturer's suggested protocol. Briefly, 10,000 SP, NSP, or CE cells were pelleted by centrifugation and resuspended in CHAPS XL lysis buffer. The reaction mixtures containing the cell lysates were then incubated for 60 minutes at 37°C and subjected to PCR. PCR consisted of 30 cycles at 94°C for 30 seconds, 56°C for 30 seconds, and 72°C for 1 minute. Reaction mixtures were then subjected to electrophoresis on a 10% polyacrylamide gel. After electrophoresis, the gel was stained with SYBR Green I

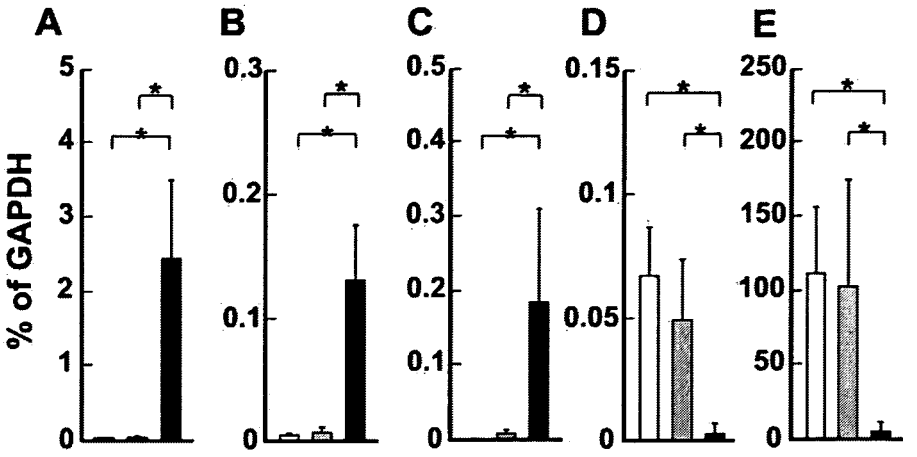

Figure 2. Quantification of mRNA in limbal epithelial side-population (SP) and non-SP (NSP) cells and corneal epithelial (CE) cells. Total RNA was extracted from limbal epithelial SP cells, NSP cells, and CE cells after fluorescence-activated cell sorting and subjected to real-time quantitative reverse transcription–polymerase chain reaction. Relative expression of the selected genes was normalized to that of GAPDH for each sample. mRNA expression of ABCG2 **(A)**, Bmi-1 **(B)**, nestin **(C)**, CK 3 **(D)**, and CK 12 **(E)** is shown. Expression levels were determined from SP cells (black bar), NSP cells (gray bar), and CE cells (white bar) for each individual mRNA. Data represent the mean value from four to six samples. Error bars indicate the standard deviation (*$p < .01$).

(Molecular Probes, Eugene, OR, http://probes.invitrogen.com) and the image was recorded with Typhoon (Amersham Biosciences, Piscataway, NJ, http://www.amersham.com).

Results

Limbal Epithelium Contains a Side Population with Cells of Smaller Size

To determine whether SP cells were present in either the limbal or corneal epithelium, both epithelial cell types were isolated from the eyes of New Zealand white rabbits and subjected to Hoechst 33342 dye efflux assay. SP cells were nearly undetected in corneal epithelial cells (Fig. 1A; 0.01% gated cells), similar to results in human eyes [17]. In contrast, a distinct population with decreased Hoechst 33342 blue/red fluorescence was detected in limbal epithelial cells (Fig. 1B; 0.40% gated cells), also similar to previous results with human limbus [17]. Hoechst 33342 efflux was antagonized by both verapamil, an inhibitor of Hoechst 33342 dye transport, and tryprostatin A, a specific inhibitor of ABCG2 (Figs. 1C, 1D) in the same fashion as previous results using different tissues of origin [8, 11, 18, 19]. SP and NSP cell fractions were collected by cell sorting as denoted in Figure 1B, and microscopic analysis (Figs. 1E, 1F) revealed that SP cells had a smaller cell size compared with NSP cells. These results were also confirmed by forward scatter analysis using FACS (Fig. 1G).

Limbal Epithelial SP Cells Express Stem Cell–Related Genes

To examine whether SP cells have stem cell–like phenotypes, gene expression analyses of SP and NSP cells from the limbus

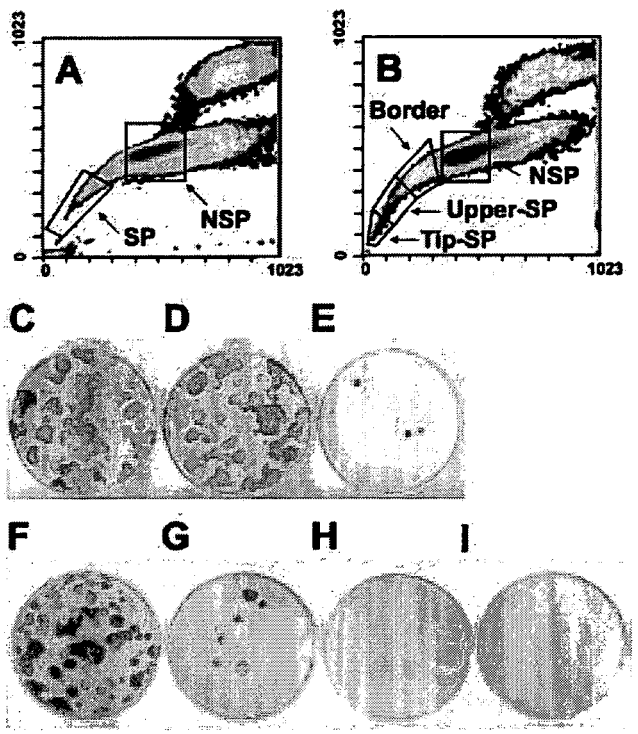

Figure 3. Colony-forming assay with limbal epithelial side-population (SP) cells and non-SP (NSP) cells. Limbal epithelial cells were separated by fluorescence-activated cell sorting into SP and NSP cells **(A)** for colony-forming assays. For in-depth analysis, limbal epithelial cells were sorted into four gates: Tip-SP, upper-SP, border, and NSP cells **(B)**. After cell sorting, viable limbal epithelial cells **(C)**, NSP cells **(D)**, or SP cells **(E)** were seeded onto mitomycin C–treated NIH-3T3 feeder layers at a density of 1,000 cells per 60-mm dish. For detailed studies, NSP cells **(F)**, border cells **(G)**, upper-SP cells **(H)**, or Tip-SP cells **(I)** were subjected to colony-forming assays under the same conditions. Cells were cultured for approximately 10 days followed by fixation and staining with rhodamine B.

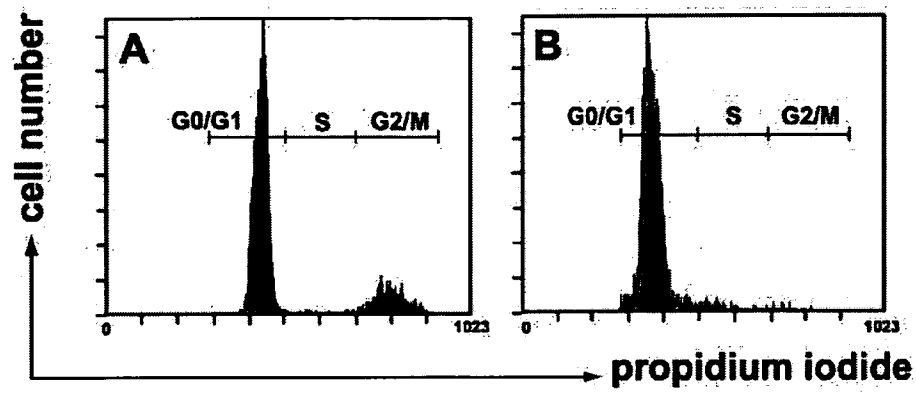

Figure 4. Cell-cycle state of limbal epithelial side-population (SP) cells. After sorting of all viable limbal epithelial cells and SP cells, cell membranes were disrupted using Nonidet P-40 followed by staining with propidium iodide. The cell-cycle phase in which each individual cell resided, from either all viable limbal epithelial cells (**A**) or SP cells (**B**), was detected by flow cytometry.

as well as CE cells were conducted using real-time quantitative RT-PCR. ABCG2, which is required to induce the SP phenotype; Bmi-1, necessary for the self-renewal of HSCs and neural stem cells [20–24]; and nestin, an intermediate filament specifically expressed in neural stem cells [25] were used as stem cell markers. Significant expression of ABCG2, Bmi-1, and nestin was detected in SP cells, but neither NSP cells nor CE cells showed expression of these genes. On the contrary, cytokeratin 3 (CK3) and cytokeratin 12 (CK12), which are known markers of differentiated CE cells [26], were significantly expressed in both NSP and CE cells but not in SP cells (Fig. 2). Additionally, results from immunostaining with anti-ABCG2 antibodies have previously revealed that ABCG2-positive cells comprise only a small portion of the human limbal epithelium, with negative staining in central corneas [17, 27].

SP Cells Are Growth Arrested in the Quiescent State

Because SP cells corresponded to a CE stem cell phenotype in location and gene expression, we investigated whether SP cells (Fig. 3A) have a strong capacity for proliferation using colony-forming assays. Unexpectedly, whereas cell fractions of all limbal epithelial cells (Fig. 3C) or NSP cells (Fig. 3D) had high proliferative capabilities, SP cells (Fig. 3E) demonstrated an extremely low colony-forming efficiency (CFE) (Table 1). Even when culture conditions were modified, such as the addition of various cytokines and growth factors, coculture with NSP cells, or isolation from wounded corneas, SP cells were still unable to form a significant number of colonies in vitro (data not shown). These results suggested that SP cells have almost no capacity for proliferation under normal in vitro culture conditions for CE cells.

To investigate the proliferative potential of limbal SP cells in greater detail, limbal epithelial cells were sorted into four gates, representing the tip-SP, upper-SP, border, and NSP cells (Fig. 3B). Results from colony-forming assays showed that whereas NSP cells (Fig. 3F) had a CFE comparable to all limbal epithelial cells, border (Fig. 3G), upper-SP (Fig. 3H), and tip-SP (Fig. 3I) cells all had negligible CFEs compared with NSP cells (Table 1). Therefore, the colony-forming ability of limbal epithelial cells is likely nearly completely derived from the NSP cell fraction.

Because SP cells demonstrated almost no proliferative capabilities in vitro, we investigated the cell-cycle state of SP cells. After sorting of SP cells and viable limbal epithelial cells, each cell fraction was permeabilized and stained with propidium iodide, followed by flow cytometric analysis. Although the cell cycle of limbal epithelial cells was promoted with active cell division, SP cells were nearly all growth arrested in G0/G1 (Fig. 4, Table 2).

Results from colony-forming assays (Fig. 3, Table 1) and cell-cycle analysis (Fig. 4, Table 2) suggested that SP cells may represent a quiescent stem cell population. To confirm this possibility, we examined telomerase activity in SP cells using

Table 1. Colony-forming efficiencies and detailed analysis of limbal epithelial cells subjected to Hoechst 33342 exclusion assays

	Viable cells (%)	CFE (%)
All	—	8.49 ± 3.03
NSP	66.1 ± 3.92	7.75 ± 2.42
SP	0.40 ± 0.19	0.38 ± 0.09
Border	2.83 ± 0.55	0.83 ± 0.15
Upper SP	0.20 ± 0.04	0.10 ± 0.10
Tip SP	0.03 ± 0.01	ND

Epithelial cells subjected to fluorescence-activated cell sorting were sorted, and the corresponding percentages of cells in each gate from Figures 3A and 3B are presented. Additionally, colony-forming efficiencies for cells from each gate are shown. Values are presented as means± standard deviations.

Abbreviations: CFE, colony-forming efficiency; ND, not determined.

Table 2. Cell-cycle state of limbal epithelial side-population cells

	G0/G1	S	G2/M
SP	96.9 ± 0.6	1.1 ± 0.3	1.6 ± 0.4
All	78.6 ± 2.5	3.2 ± 0.8	18.4 ± 1.7

Values correspond to the percentage of cells in each cell-cycle phase. Values are presented as means ± standard deviations.

the TRAP assay. It has been previously reported that quiescent stem cells have no telomerase activity but that it is upregulated in actively proliferating TA and progenitor cells in hair follicles [28], skin [29], and bone marrow [30]. Cell lysates from each cell fraction purified by FACS were reacted to lengthen telomeres, followed by amplification of the product with PCR. HeLa cells were used as a positive control, and each cell fraction was also treated with heat as a negative control. We found that both SP and CE cells had no telomerase activity, whereas NSP cells demonstrated weak activity (Fig. 5).

Discussion

Limbal Epithelial SP Cells Resemble Other Adult Tissue-Specific Stem Cells

In the present study, we demonstrated that limbal epithelial SP cells have HSC-like properties, including small size, increased expression of the stem cell markers ABCG2, Bmi-1, and nestin, and an SP phenotype. Immature cell types such as stem cells are thought to be much smaller in size compared with normal cells, and limbal epithelial SP cells were significantly smaller than NSP cells and appeared more immature and simple in cell shape, thus supporting the view that SP cells represent a CE stem cell population or, at the very least, an extremely immature cell population.

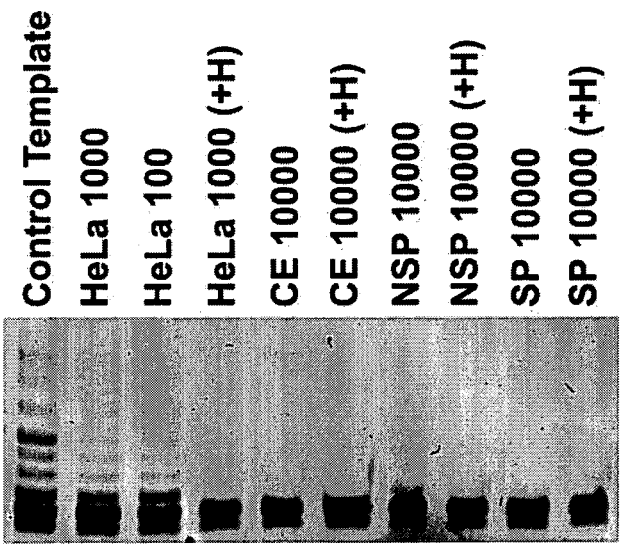

Figure 5. Telomerase activity. After cell sorting, telomerase activity was examined by the telomeric repeat amplifying protocol (TRAP) assay for each cell fraction. A control template, containing several telomeric repeats, was used at a concentration of 0.2 mol/μl. HeLa cells were selected as a positive control. Each cell lysate was also treated with heat (+H) as a negative control. After TRAP assay, each reaction mixture was subjected to polyacrylamide electrophoresis followed by staining with SYBR green I. The number of cells used for each sample is shown. Abbreviations: CE, corneal epithelial; NSP, non-side population; SP, side population.

For the SP phenotype to be indicative of stem cell–like properties, the expression of ABCG2 is required [7, 31, 32]. Because adult stem cells are known to be particularly resistant to various stresses, the expression of ABCG2 likely acts as a protective mechanism, allowing for the efflux of various soluble factors or toxins that could result in the premature differentiation of SP cells.

Bmi-1, a member of the polycomb gene family, is expressed not only in HSCs but also in neural stem cells and is vital to the self-renewal of adult stem cells [20–24]. The increased expression of Bmi-1 in limbal epithelial SP cells therefore also seems likely to be critically involved in the self-renewal of CE stem cells. Bmi-1 decreases expression of p16 and p19 [20, 21, 33], known cyclin-dependent kinase inhibitors, and increases telomerase activity [34]. However, even though Bmi-1 is believed to promote increased proliferation of cells, higher expression of Bmi-1 has been correlated with the maintenance of the stem cell phenotype. It seems that adult stem cells have high proliferative potential, but other regulatory factors act to prevent unnecessary proliferation and carefully regulate the generation of differentiated progeny.

Nestin, an intermediate filament protein and known neural stem cell marker [25], was also more highly expressed in SP cells compared with other cell fractions. Increased nestin expression has previously been detected in SP cells isolated from other tissues, such as the pancreas [19] and retina [18], and may therefore be a characteristic cytoskeletal molecule of not only neural stem cells but also other adult stem cells with the SP phenotype.

Therefore, the previously proposed environment of the basal layer, being the most isolated from the exposed ocular surface, in conjunction with the expression of the stem cell markers ABCG2, Bmi-1, and nestin, may allow for the proper maintenance and self-renewal of limbal epithelial SP cells.

SP Cells Likely Represent a Quiescent Stem Cell Population in the Limbal Epithelium

In the present study, most limbal epithelial SP cells were found to be growth arrested in G0/G1, compared with all cells isolated from the limbal epithelium. HSCs are known to be quiescent in the bone marrow niche [1, 35], and limbal epithelial SP cells therefore also resemble HSCs by being cell-cycle arrested. The

quiescent state of limbal epithelial SP cells led to the interesting finding that SP cells did not proliferate and could not create colonies in vitro, like previously defined epithelial stem cells. Whereas tip-SP cells revealed no colony formation, very low CFEs were observed for the SP, upper-SP, and border-gated cells (Table 1). These values, however, seem correlated with the purity of the SP fraction after cell sorting, because SP cells isolated by FACS inevitably contain approximately 1%–2% contamination by other cells (data not shown). Therefore, it is believed that the observed CFE is likely due to contamination by NSP cells, which account for the proliferative capabilities of all cells in the limbal epithelium. Moreover, SP cells showed lower expression of $\alpha 6$ and $\beta 1$ integrins (data not shown), which are known to be highly expressed in cells with strong proliferative capabilities [36–38].

Although a recent study reported that limbal epithelial SP cells had the ability to form colonies [39], their experimental procedures had several different conditions. In particular, the seeded cell density, UV laser intensity used for FACS, and primary cell culture before cell sorting were most likely the cause for the conflicting results. In their colony-forming assay, epithelial cells were seeded at a density that was 20 times higher than in the present study. Therefore, even though scanned images revealed dish surfaces that were nearly completely covered by proliferating cells, results actually showed significantly lower CFEs (4% for SP and 1% for NSP cells) compared with our present results (approximately 10% for NSP cells). Although these differences may be due to culture conditions that are better suited for limbal epithelial cells, we also confirmed that the proliferative capacity of limbal epithelial cells was markedly decreased, with CFEs comparable to their results, when UV laser power was greater than 50 mW (data not shown). In their study, a laser intensity of 100 mW was used, which can cause significant damage to cells during sorting and may result in diminished proliferative abilities. Additionally, the effects of cultured cells in their study, as opposed to freshly isolated cells, used for FACS in the present case, cannot be excluded. We have, in fact, observed that no SP cells were detected when primary cultured cells were sorted (data not shown), a result that supports our finding that SP cells are growth arrested in vitro.

It has previously been shown that cells that are in active proliferation, such as TA or progenitor cells, but not quiescent adult stem cells, have telomerase activity [28–30]. It is thought that upregulation of telomerase occurs upon differentiation into progenitor or TA cells to prevent the rapid depletion of telomeres during cell division. This process is transient, with telomerase activity decreasing upon the formation of fully differentiated progeny [30]. The corneal epithelium has a relatively short span of renewal, similar to bone marrow, skin, and hair follicles, and therefore the telomerase activity present in the NSP cell fraction likely corresponds to cells that are in active proliferation, such as progenitor or TA cells. Limbal SP cells that have neither telomerase activity nor expression of the differentiated cell markers CK3 and CK12 therefore seem to represent a quiescent stem cell population. NSP cells, which have increased telomerase activity and are clonogenic, likely consist of both TA and progenitor cells that are actively proliferating but not quiescent stem cells, due to both mitotic activity and expression of differentiated CE markers. Finally, CE cells, which express CK3 and CK12, are thought to be highly differentiated cells that express CK3 and CK12, in which telomerase activity has been downregulated because of the loss of proliferative potential.

Our results demonstrate that limbal epithelial SP cells have stem cell–like properties, including growth arrest in the quiescent state, thus meeting the criteria of adult stem cells. It is currently accepted that epithelial stem cells are slow cycling and demonstrate high proliferative potential. However, limbal epithelial SP cells are cell-cycle arrested and, due to their quiescent state, exhibit no in vitro proliferative capabilities. It therefore seems that previously defined epithelial stem cells via colony-forming assays or detection of label-retaining cells may not represent true stem cells, but rather immature progenitor cells. In fact, Oshima et al. [40], discussing their results on adult multipotent stem cells from hair follicles, state that these cells, with high proliferative potential, are likely generated from more immature stem cells.

To accurately identify epithelial stem cells, it seems important to meet the criteria used for other adult stem cells, such as HSCs. The current view is that epithelial stem cells, which demonstrate high proliferative capacity and slow cell cycle, give rise to TA cells, which have a limited number of cell divisions, and finally generate differentiated progeny. We now believe that limbal epithelial SP cells represent an epithelial stem cell population that resides in the quiescent state in the basal layer of the limbus. We also theorize that limbal epithelial SP cells generate progenitor or "active" stem cells that are mitotically cycling and have high proliferative potential. It is these progenitor cells that comprise the portion of the NSP fraction that have active telomerase, demonstrate a slow cell cycle, and have colony-forming abilities. Under normal epithelial cell culture conditions, these colony-forming progenitor cells can proliferate to produce more differentiated cells that can form stratified epithelial layers. CE progenitor cells may therefore be analogous to the multipotent progenitor cells of the hematopoietic system and generate TA cells that are present in the NSP cell fraction of the limbus and can also migrate toward the central cornea to produce the CE cells that express CK3 and CK12. Epithelial stem cells should therefore be defined not by markers of clonogenic or label-retaining cells but by markers of adult stem cells, such

as the SP phenotype via expression of ABCG2; Bmi-1, which regulates stem cell self-renewal; the expression of nestin found in various SP and stem cell populations; and the absence of telomerase activity, representing the cell-cycle arrest of quiescent stem cells.

Previously, we and others have shown the successful clinical transplantation of ex vivo–expanded limbal epithelial cells to human patients [41]. In such cases, the understanding of CE stem cells is of vital importance to the long-term survival of transplanted cells and may contribute to a higher quality of transplantation. However, unlike in the hematopoietic system, where there is an established and accepted in vivo reconstitution assay, the current lack of an analogous model for the corneal epithelial system makes it difficult to confirm the abilities for self-renewal and long-term maintenance of limbal epithelial SP cells. It seems likely, however, that the understanding of the mechanisms that control the proliferation and differentiation of limbal epithelial SP cells will have a significant influence on successful applications in the clinical setting.

ACKNOWLEDGMENTS

We thank Dr. Ai Kushida (Tokyo Women's Medical University) for her technical review and useful comments. This work was supported by Grants-in-Aid for Scientific Research (15390530, 16200036, and 16300161); the High-Tech Research Center Program; the Center of Excellence Program for the 21st Century from the Ministry of Education, Culture, Sports, Science, and Technology in Japan; and the Core Research for Evolution Science and Technology from the Japan Science and Technology Agency.

DISCLOSURES

The authors indicate no potential conflicts of interest.

REFERENCES

1 Arai F, Hirao A, Ohmura M et al. Tie2/angiopoietin-1 signaling regulates hematopoietic stem cell quiescence in the bone marrow niche. Cell 2004;118:149–161.

2 Goodell MA, Brose K, Paradis G et al. Isolation and functional properties of murine hematopoietic stem cells that are replicating in vivo. J Exp Med 1996;183:1797–1806.

3 Zhou S, Schuetz JD, Bunting KD et al. The ABC transporter Bcrp1/ABCG2 is expressed in a wide variety of stem cells and is a molecular determinant of the side-population phenotype. Nat Med 2001;7:1028–1034.

4 Bunting KD. ABC transporters as phenotypic markers and functional regulators of stem cells. STEM CELLS 2002;20:11–20.

5 Kim M, Turnquist H, Jackson J et al. The multidrug resistance transporter ABCG2 (breast cancer resistance protein 1) effluxes Hoechst 33342 and is overexpressed in hematopoietic stem cells. Clin Cancer Res 2002;8:22–28.

6 Scharenberg CW, Harkey MA, Torok-Storb B. The ABCG2 transporter is an efficient Hoechst 33342 efflux pump and is preferentially expressed by immature human hematopoietic progenitors. Blood 2002;99:507–512.

7 Zhou S, Morris JJ, Barnes Y et al. Bcrp1 gene expression is required for normal numbers of side population stem cells in mice, and confers relative protection to mitoxantrone in hematopoietic cells in vivo. Proc Natl Acad Sci U S A 2002;99:12339–12344.

8 Uchida N, Leung FY, Eaves CJ. Liver and marrow of adult mdr-1a/1b(-/-) mice show normal generation, function, and multi-tissue trafficking of primitive hematopoietic cells. Exp Hematol 2002;30:862–869.

9 Shimano K, Satake M, Okaya A et al. Hepatic oval cells have the side population phenotype defined by expression of ATP-binding cassette transporter ABCG2/BCRP1. Am J Pathol 2003;163:3–9.

10 Jackson KA, Mi T, Goodell MA. Hematopoietic potential of stem cells isolated from murine skeletal muscle. Proc Natl Acad Sci U S A 1999;96:14482–14486.

11 Summer R, Kotton DN, Sun X et al. Side population cells and Bcrp1 expression in lung. Am J Physiol Lung Cell Mol Physiol 2003;285:L97–104.

12 Schermer A, Galvin S, Sun TT. Differentiation-related expression of a major 64K corneal keratin in vivo and in culture suggests limbal location of corneal epithelial stem cells. J Cell Biol 1986;103:49–62.

13 Cotsarelis G, Cheng SZ, Dong G et al. Existence of slow-cycling limbal epithelial basal cells that can be preferentially stimulated to proliferate: implications on epithelial stem cells. Cell 1989;57:201–209.

14 Kinoshita S, Friend J, Thoft RA. Sex chromatin of donor corneal epithelium in rabbits. Invest Ophthalmol Vis Sci 1981;21:434–441.

15 Thoft RA, Friend J. The X, Y, Z hypothesis of corneal epithelial maintenance. Invest Ophthalmol Vis Sci 1983;24:1442–1443.

16 Buck RC. Measurement of centripetal migration of normal corneal epithelial cells in the mouse. Invest Ophthalmol Vis Sci 1985;26:1296–1299.

17 Watanabe K, Nishida K, Yamato M et al. Human limbal epithelium contains side population cells expressing the ATP-binding cassette transporter ABCG2. FEBS Lett 2004;565:6–10.

18 Bhattacharya S, Jackson JD, Das AV et al. Direct identification and enrichment of retinal stem cells/progenitors by Hoechst dye efflux assay. Invest Ophthalmol Vis Sci 2003;44:2764–2773.

19 Lechner A, Leech CA, Abraham EJ et al. Nestin-positive progenitor cells derived from adult human pancreatic islets of Langerhans contain side population (SP) cells defined by expression of the ABCG2 (BCRP1) ATP-binding cassette transporter. Biochem Biophys Res Commun 2002;293:670–674.

20 Molofsky AV, Pardal R, Iwashita T et al. Bmi-1 dependence distinguishes neural stem cell self-renewal from progenitor proliferation. Nature 2003;425:962–967.

21 Park IK, Qian D, Kiel M et al. Bmi-1 is required for maintenance of adult self-renewing haematopoietic stem cells. Nature 2003;423:302–305.

22 Raaphorst FM. Self-renewal of hematopoietic and leukemic stem cells: a central role for the Polycomb-group gene Bmi-1. Trends Immunol 2003;24:522–524.

23 Iwama A, Oguro H, Negishi M et al. Enhanced self-renewal of hematopoietic stem cells mediated by the polycomb gene product Bmi-1. Immunity 2004;21:843–851.

24 Zhang P, Iwasaki-Arai J, Iwasaki H et al. Enhancement of hematopoietic stem cell repopulating capacity and self-renewal in the absence of the transcription factor C/EBP alpha. Immunity 2004;21:853–863.

25 Lendahl U, Zimmerman LB, McKay RD. CNS stem cells express a new class of intermediate filament protein. Cell 1990;60:585–595.

26 Chaloin-Dufau C, Sun TT, Dhouailly D. Appearance of the keratin pair K3/K12 during embryonic and adult corneal epithelial differentiation in the chick and in the rabbit. Cell Differ Dev 1990;32:97–108.

27 Wolosin JM, Budak MT, Akinci MA. Ocular surface epithelial and stem cell development. Int J Dev Biol 2004;48:981–991.

28 Ramirez RD, Wright WE, Shay JW et al. Telomerase activity concentrates in the mitotically active segments of human hair follicles. J Invest Dermatol 1997;108:113–117.

29 Bickenbach JR, Vormwald-Dogan V, Bachor C et al. Telomerase is not an epidermal stem cell marker and is downregulated by calcium. J Invest Dermatol 1998;111:1045–1052.

30 Chiu CP, Dragowska W, Kim NW et al. Differential expression of telomerase activity in hematopoietic progenitors from adult human bone marrow. STEM CELLS 1996;14:239–248.

31 Triel C, Vestergaard ME, Bolund L et al. Side population cells in human and mouse epidermis lack stem cell characteristics. Exp Cell Res 2004; 295:79–90.

32 Terunuma A, Jackson KL, Kapoor V et al. Side population keratinocytes resembling bone marrow side population stem cells are distinct from label-retaining keratinocyte stem cells. J Invest Dermatol 2003;121: 1095–1103.

33 Smith KS, Chanda SK, Lingbeek M et al. Bmi-1 regulation of INK4A-ARF is a downstream requirement for transformation of hematopoietic progenitors by E2a-Pbx1. Mol Cell 2003;12:393–400.

34 Milyavsky M, Shats I, Erez N et al. Prolonged culture of telomerase-immortalized human fibroblasts leads to a premalignant phenotype. Cancer Res 2003;63:7147–7157.

35 Moore KA, Lemischka IR. "Tie-ing" down the hematopoietic niche. Cell 2004;118:139–140.

36 Li A, Simmons PJ, Kaur P. Identification and isolation of candidate human keratinocyte stem cells based on cell surface phenotype. Proc Natl Acad Sci U S A 1998;95:3902–3907.

37 Zhu AJ, Haase I, Watt FM. Signaling via beta1 integrins and mitogen-activated protein kinase determines human epidermal stem cell fate in vitro. Proc Natl Acad Sci U S A 1999;96:6728–6733.

38 Jones PH, Watt FM. Separation of human epidermal stem cells from transit amplifying cells on the basis of differences in integrin function and expression. Cell 1993;73:713–724.

39 de Paiva CS, Chen Z, Corrales RM et al. ABCG2 transporter identifies a population of clonogenic human limbal epithelial cells. STEM CELLS 2005;23:63–73.

40 Oshima H, Rochat A, Kedzia C et al. Morphogenesis and renewal of hair follicles from adult multipotent stem cells. Cell 2001;104:233–245.

41 Nishida K, Yamato M, Hayashida Y et al. Functional bioengineered corneal epithelial sheet grafts from corneal stem cells expanded ex vivo on a temperature-responsive cell culture surface. Transplantation 2004; 77:379–385.

Key Engineering Materials Vols. 309-311 (May 2006) pp. 263-266
online at http://www.scientific.net

Cytotoxicity of Various Calcium Phosphate Ceramics

Masato Tamai[1a], Ryusuke Nakaoka[1b] and Toshie Tsuchiya[1c]
Division of Medical Devices, National Institute of Health Science
1-18-1 Kamiyoga, Setagaya-ku, Tokyo 158-8501 Japan
[a]m-tamai@nihs.go.jp, [b]nakaoka@nihs.go.jp, [c]tsuchiya@nihs.go.jp

Keywords: Calcium phosphate ceramics, Cytotoxicity,

Abstract. The cytotoxicity of five calcium phosphate ceramics, hydroxyapatite (HAp), flouroapatite (FAp), α-tricalcium phosphate (α-TCP), β-tricalcium phosphate (β-TCP) and tetracalcium phosphate (TTCP), was investigated. Based on the guidelines of biological test for medical devices in Japan, a cytotoxicity test of these calcium phosphates was carried out using Chinese hamster V79 lung fibroblasts. The cytotoxic study revealed that FAp and α-TCP showed high cytotoxicities. From various analyses, it was considered that the cytotoxicity of the FAp was due to fluorine ions extracted in a culture medium and the cytotoxicity of α-TCP resulted from a decrease in pH of the medium by the phosphoric acid, which produced by hydrolysis of the α-TCP.

Introduction

From the view point of biological affinity to bone, calcium phosphate (CP) ceramics have been studied to utilize for many purposes in a medical field. For instance, hydroxyapatite ($Ca_{10}(PO_4)_6(OH)_2$, HAp) and β-tricalcium phosphate (β-$Ca_3(PO_4)_2$, ß-TCP), are known to be biologically bonded to natural bones and their porous materials have been studied for effective restoration of bone defects.[1,2] Fluoroapatite ($Ca_{10}(PO_4)_6F_2$, FAp) has been reported to have a potential of novel bone repairing materials with high stability *in vivo*, since solubility of FAp is lower than that of HAp.[3,4] In addition, CP cement is also promising for bone repair and it is well known that α-tricalcium phosphate (α-$Ca_3(PO_4)_2$, α-TCP) and tetracalcium phosphate ($Ca_4(PO_4)_2O$, TTCP) are starting materials for the harden reaction of the bone cement.[5,6]

To develop biomaterials for utilizing for bone tissue, various properties, e.g. biological, physical and chemical property, should be satisfied. Among them, biological safety is important for the biomaterials. Since only a few studies which discuss the cytotoxicity of calcium phosphate ceramics have been reported, the cytotoxicity of CP ceramics is worthy to be investigated in order to design bioceramics with good biological safety for medical application. Therefore, the cytotoxicities of five calcium phosphate ceramics, hydroxyapatite (HAp), flouroapatite (FAp), α-tricalcium phosphate (α-TCP), β-tricalcium phosphate (β-TCP) and tetracalcium phosphate (TTCP) were investigated.

Materials and Methods

Materials

Five kinds of CP ceramics, HAp, FAp, α-TCP, β-TCP and TTCP were purchased from Wako chem. Co. Ltd. CP powders (0.25 g) was put into stainless mold and uniaxially pressed at 30MPa for 1 min to form a pellet. The dimensions of the obtained CP pellet were 1mm in thickness and 12mm in diameter. CP pellets were sterilized by an autoclave at 121°C for 20 min.

Cytotoxicty test on CP ceramics

Cytotoxicity test was carried out using Chinese hamster V79 lung fibroblasts by a colony assay system. V79 cells were maintained in Eagle's minimum essential medium (Nissui Pharmaceutical Co. Ltd.) with 10% fetal calf serum (FCS, Intergen Co. Ltd.) and incubated at 37 °C in a humidified atmosphere with 5% CO_2.

The method of cell seeding in the cytotoxicity test of CP ceramics was shown below; each CP pellets were placed in each culture wells of 24 well culture plates (Corning Co. Ltd.) and 300μl of culture medium was added into each well. Then, 50 cells/300μl of the cell suspension in the

culture medium were added into each well and incubated at 37°C for 4 h. Finally, 400μl of the culture medium was added into each well and the plates were incubated at 37 °C in a humidified atmosphere with 5 % CO_2 for 7days. In order to investigate a cell adhesive property on the CP ceramics, the culture medium was changed after 4 h and further incubated for 7days. The removed culture medium was transferred to another well of a new plate and incubated for 7days as well.

Cytotoxicity of extracts from CP ceramics was also investigated in this study. Suspensions of CP ceramics in the culture medium (100mg/mL) were stirred at 37°C for 3days under the rotation condition at 150rpm. The suspensions were centrifuged and the supernatants were collected as test extracts. In addition, media with various pH values were prepared using HCl solution to investigate an effect of pH on cell survival. Fifty V79 cells in 1ml of the extracts or the medium with different pH value were incubated at 37 °C for 7days.

After 7-day incubation, the cells were fixed in methanol and the number of the V79 colonies was counted after staining cells with 5%-Giemsa solution to estimate the cytotoxicity of the test sample. In addition, the pH of the medium after 7-days culture was measured to estimate the effect of the pH of the medium on the cytotoxicity test.

Characterization of CP ceramics

The structural changes of CP before and after an autoclave-sterilization or an incubation at 37°C culture were investigated by powder X-ray diffraction (XRD) analysis and scanning electron microscopy (SEM). XRD analysis was carried out (Rigaku Co., Ltd. / RINT 2000) with the CuK_α radiation at 40kV, 50mA. SEM observations were performed (JEOL / JSM-5800LV) with an accelerating voltage of 25kV.

Results and Discussion

Cytotoxicity of various CP ceramics

From XRD analysis, no structural changes of CPs were observed after an autoclave sterilization. After staining CP pellets, it was observed that cell colonies were formed on various CP ceramics pellets (Fig.1(a)). The results of the cytotoxicity test of CPs are shown in Fig.1(b). The cell colonies were hardly formed on FAp and α-TCP pellets and the ratios of the colonies formed on these pellets against V79-alone culture were 22.6% and 0.0%, respectively. In addition, the ratios of the colonies on the HAp, β-TCP and TTCP pellets were 58.1%, 57.3% and 78.4%, respectively. As no colonies were observed after 7-day culture of the removed medium in cell adhesion studies of CP ceramics, these results suggested that V79 cells can adhere and be viable on these pellets, irrespective of the type of CP ceramics. Figure 2 shows the formation of colonies cultured in extract from CP ceramics. The cytotoxicity test of extracts from CPs revealed that the tendency of their cytotoxicities was similar to that of the cytotoxicities on the respective CP pellets themselves (Fig.1(b)).

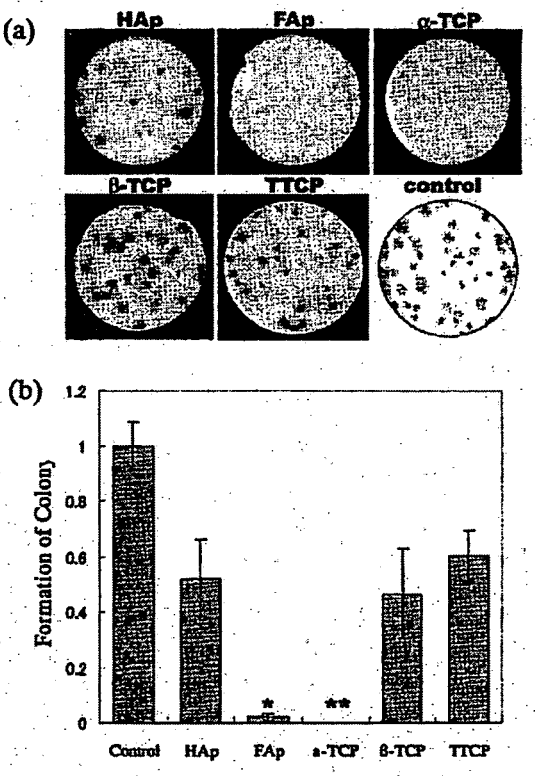

Fig.1. The appearance of colonies on various CP pellets (a) and their colony formation ratios (b). (*p<0.05 against for V79 alone, **p<0.01 against for V79 alone)

The fact that less formation of colonies was observed on FAp and α-TCP pellets suggests that they are highly cytotoxic. In addition to results shown in Fig.2, it is suggested that the differences in the colony formation ratio on various CP pellets are ascribed to difference in extract properties from the CP, which may be related with the composition or crystal structure. As shown in Table 1, the pH of culture medium after incubation with FAp pellets is almost the same as that of HAp, while the pH of the α-TCP-incubated medium is much lower than that of the other CP ceramics-incubated media.
In order to consider the reason of the low pH of the a-TCP-incubated medium, a surface structural change of α-TCP before and after incubation was analyzed by SEM. SEM images of α-TCP before and after extraction treatment are shown in Fig.3. Before extraction, a particle size of α-TCP was about 10μm and its surface was smooth (Fig.3(a) and (b)). However, whisker-like precipitates of 1-2μm in length and 2-300nm in width were observed at the surface of α-TCP after the extraction, although there was no change in its particle size (Fig.3(c) and (d)). It is well known

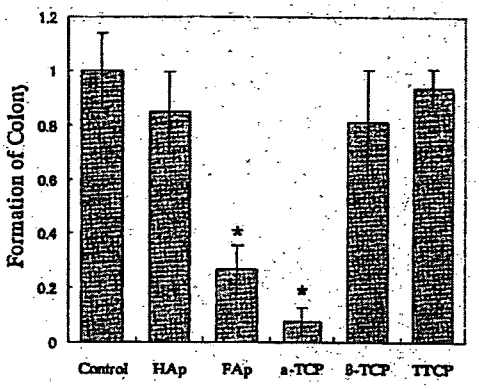

Fig.2. Formation of colony cultured in extract from various CP ceramics. (*p<0.01 against for V79 alone)

Table 1. The pH and Ca concentration of culture medium after incubation.

Samples	pH of medium after culturing	Ca concentration /ppm
V79 alone	7.12	-
HAp	7.24	0.19
FAp	7.20	0.17
α-TCP	6.76	72.62
β-TCP	7.40	1.27
TTCP	7.65	0.58

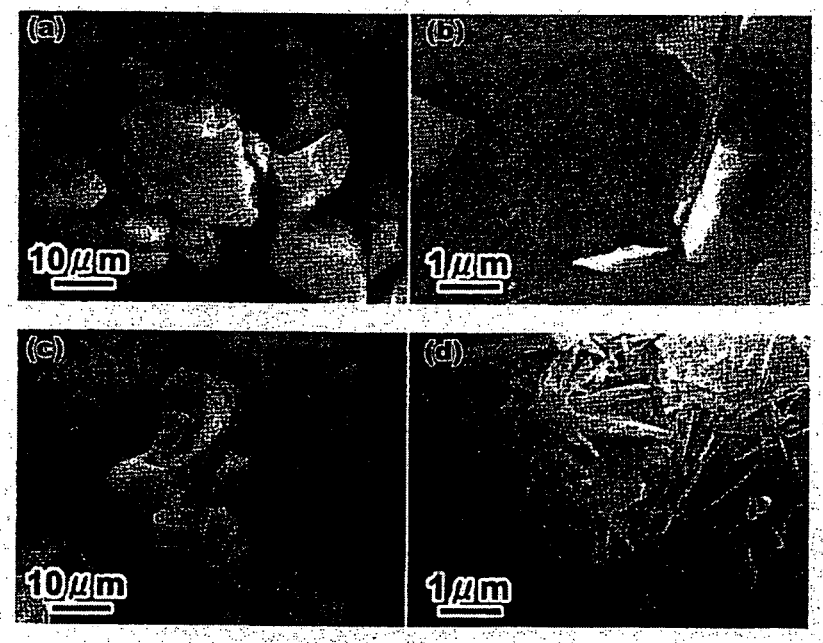

Fig.3. SEM images of α-TCP before (a), (b) and after extract treatment (c), (d). (a) and (c) are whole image of before and after extract treatment, respectively. (b) and (d) are enlarged image of the area enclosed by a rectangle in (a) and (c), respectively.

that calcium phosphates convert to HAp in aqueous solution with high pH value. Since the solubility of α-TCP is higher than that of other calcium phosphates, α-TCP rapidly converts to HAp as follows;

$$10Ca_3(PO_4)_2+6H_2O \rightarrow 3Ca_{10}(PO_4)_6(OH)_2+2H_3PO_4$$

According to the report of this conversion [7], HAp produced by the above reaction has whisker-like morphology. Therefore, the whisker-like precipitates in Fig.3 (d) can be regarded as HAp, so that it is considered that the above conversion occurs at the surface of the α-TCP during incubation.

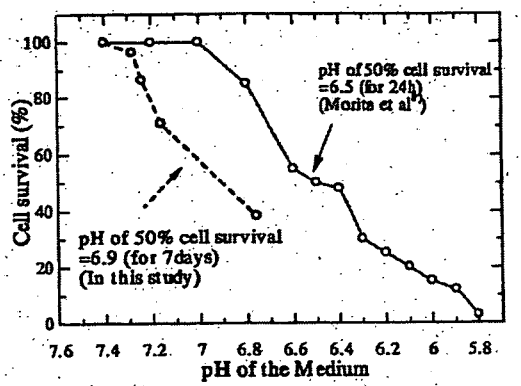

Fig.4. V79 cell survival in the medium with various pH values.

In this case, phosphoric acid is produced as a byproduct in the conversion reaction and the phosphoric acid causes the decrease in pH of the solution. As shown in Fig.4, Morita and co-workers[8] have reported that low pH itself could be clastogenic to mammalian cells and the pH of 50% V79 cell survival was 6.5 for 24h incubation. In the present colony assay system, the pH of 50% V79 cell survival was 6.9 for 7-days incubation. In addition, we confirmed that phosphoric acid showed no or weak cytotoxicities under our present experimental conditions. Therefore, it is suggested that the cytotoxicity of α-TCP is mainly due to the pH decrease resulting from an increase of the phosphoric acid ion by the hydrolysis conversion from α-TCP to HAp.

On the other hand, FAp has the same crystal structure of HAp but the hydroxyl ions in HAp substituted by fluorine ions. Since it is probable that difference of the colony formation on various CP ceramics are due to eluted substances from CP as described above, the cytotoxicity of FAp would be due to eluted fluoride ions from FAp. In conclusion, this study has revealed that FAp and α-TCP have a cytotoxicity, while TTCP has lower cytotoxicity than other calcium phosphates. To develop biomaterials made from calcium phosphate, further studies are necessary to clarify their cytotoxic mechanisms.

Acknowledgment

This study was supported in part by a Grant-in-Aid for Scientific Research on Advanced Medical Technology from Ministry of Labour, Health and Welfare, Japan and a Grant-in-Aid from Japan Human Sciences Foundations.

References

[1]Y.Ito, N.Tanaka, Y.Fujimoto, Y.Yasunaga, O.Ishida, M.Agung and M.Ochi: J. Biomed. Mater. Res. Vol.69A (2004), p.454
[2]Y.Wang, T.Uemiura, J.Dong, J.Tanaka and T.Tateishi: Tissue Eng. Vol.9 (2003), p.1205
[3]S.M.Barinov, F.Rustichelli, P.V.Orlovskii, A.Lodini, S.Oscarsson, A.S.Firstov, V.S.Tumanov, P.Millet and A.Rosengren: J.Mater.Sci:Mater in Med. Vol.15 (2004), p.291
[4]K.Cheng, W.Weng, H.Qu, P.Du, G.Shen, G.Han, J.Yang and M.J.Ferreira: J. Biomed. Mater. Res. B Vol 69 (2004), p.33
[5]E.L.Carey, H.H.Xu, G.C.Simon, S.Takagi and C.L.Chow: Biomaterials Vol 26 (2005), P.5002
[6]M.E.Ooms, J.G.C.Wolke, J.P.C.M.Waerden and J.A.Jansen: J. Biomed. Mater. Res.Vol.61 (2002), p.9
[7]M.Tamai, T.Isshiki, K.Nishio, M.Nakamura, A.Nakahira and H.Endoh: J. Mater. Res. Vol.18 (2003), p.2633
[8]T.Morita, T.Nagaki, I.Fukuda and K.Okumura: Muta. Res. Vol.268 (1992), p.297

Key Engineering Materials Vols. 309-311 (May 2006) pp. 97-100
online at http://www.scientific.net

Novel Calcium Phosphate Ceramics : The Remarkable Promoting Action on the Differentiation of the Normal Human Osteoblasts

Masato Tamai[1a], Ryusuke Nakaoka[1b], Kazuo Isama [1c] and Toshie Tsuchiya[1d]
[1]Division of Medical Devices, National Institute of Health Sciences,
1-18-1 Kamiyoga, Setagaya-ku, Tokyo 158-8501 Japan
[a]m-tamai@nihs.go.jp, [b]nakaoka@nihs.go.jp, [c]isama@nihs.go.jp, [d]tsuchiya@nihs.go.jp

Keywords: Hydroxyapatite, Niobium ion, Osteoblast, Alkaline phosphatase activity

Abstract.
To promote the activity of normal human osteoblasts (NHOst), the novel HAp ceramics containing Nb ions (NbHAp) were synthesized by wet chemical process, which reacting aqueous solution containing a mixture of $Ca(NO_3)_2$, $(NH_4)_2HPO_4$, and the Nb aqueous solution. X-ray diffraction patterns indicated that NbHAp had a monolithic apatitic structure, although crystallite decreased as Nb content increased. From inductively coupled plasma analysis, maximum amount of Nb ions in the sample was almost 8.2atom% of P ions. The NbHAps were presented as aggregates and composed of fine crystal of <1μm in diameter. Nb ions in NbHAp were uniformly distributed in the aggregates. Furthermore, high-resolution XPS spectra of Nb $3d_{5/2}$ indicated that Nb ions in the HAp were presented as Nb^{5+}. These results suggested that Nb ions were at PO_4 site in crystal structure of HAp. When NHOst were cultured with the NbHAp, their ALP activity were twice as much as that of NHOst cultured with HAp without Nb ions.

Introduction

Tissue engineering takes advantages of the combined use of cultured living cells and scaffolds to deliver vital cells to the damaged site of the patient. Some tissue engineering approaches have been devised to repair large bone defect. In developing of the scaffold for bone tissue, the interaction between osteoblasts cells and scaffolds are much important. To achieve the restoration the bone tissue at early stage, the scaffold is required to have the ability of promoting proliferation and mineralization.

It is well known that hydroxyapatite ($Ca_{10}(PO_4)_6(OH)_2$, HAp) ceramics can be biologically bonded to natural bones and have been studied to utilize as the scaffolds. In addition, the structure is very tolerant of ionic substitutions and Ca^{2+} ions, PO_4^{3-} ions and OH^- ions can be replaced by various cationic or anionic ions, partly or completely[1]. For example, K^+, Mg^{2+} and Sb^{3+}, can substituted for Ca ions and CO_3^{2-} and VO_4^{3-} can substituted for PO_4^{3-} ions, completely or partially. Thus various kinds of ion substitutions can be made to synthesize novel modified-HAps.

Recently, our co-workers reported that niobium (Nb) ions have the significant effect which promotes the proliferation and differentiation of normal human osteoblastic cells (NHOst)[2]. In the present study, therefore, we attempted to synthesize the novel HAp ceramics containing Nb ions (NbHAp) to promote the activity of NHOst and investigated the interaction between NbHAp and NHOst.

Materials and Methods

Synthesis of Nb containing HAp

The NbHAp was synthesized by wet chemical process, which reacting aqueous solution containing a mixture of $Ca(NO_3)_2$, $(NH_4)_2HPO_4$, and the Nb aqueous solution. The reagent grade $Ca(NO_3)_2$, $(NH_4)_2HPO_4$ and $NbCl_5$ (Wako Pure Chemical Industries, Ltd) were used without purification. The metal ion chemical reagent was completely dissolved in an exact amount of distilled water. The Nb aqueous solution was prepared by the mixing of distilled water and $NbCl_5$ solution, which dissolved in 5vol%-hydroxyaceton and 5vol%-2-aminoethanol[3].

0.2M-$(NH_4)_2HPO_4$ and 0.01M $NbCl_5$ solutions were mixed and stirred with a magnetic bar. The Nb/(Nb+P) molar ratio of the mixing solution was set to 0.0000, 0.0167 and 0.1667. The pH of the mixing solution was adjusted to 10 using 1N-NaOH. 0.2M-$Ca(NO_3)_2$ was slowly dropped in the mixing solution (20ml/min) The ionic content of those starting solutions are shown in table 1. The pH was monitored and the reaction was terminated at pH 10.0. After the reaction, the suspension was stirred for 24h at room temperature. The precipitates were centrifuged at 3000rpm for 5min and washed with distilled water. The obtained apatites were annealed at 800°C for 2h (heating rate: 5°C/min). In this study, those precipitates obtained by reaction of $Ca(NO_3)_2$ solution and the mixing solution with different Nb/(Nb+P) molar ratio of 0.000, 0.0167 and 0.1667 are named HAp , NbHAp-I and NbHAp-II, respectively.

Characterization of NbHAp

The NbHAps were characterized by X-ray diffraction analysis (XRD, Rigaku, Rint2000). Ca, P and Nb ions concentrations in apatites are measured by inductively coupled plasma (ICP, Hewlett-Packard, HP4500). Microstructural evaluation was performed by scanning electron microscopy (SEM) and energy dispersive X-ray spectroscopy (EDS) (JEOL, LV5800). The chemical state of Nb ions in HAp was investigated by X-ray photon spectroscopy (XPS, Shimadzu, ESCA-3200).

Osteogenesis evaluation of NHOst cultured with NbHAp

NHOst were purchased from BioWhittaker Inc.(Walkersville,MD). The NHOst were maintained in alpha minimum essential medium (αMEM, Gibco, Grand Island, NY) containing 10%-FCS in incubators at 37°C in a humidified atmosphere with 5% CO_2. All assays were performed using αMEM containing 10%-FCS supplemented with 10mM beta-glycerophosphate. NHOst cells (4×10^4 cells/well/ml) were co-cultured with 5mg of the apatites for 7days to evaluated the effects of the apatites on NHOst.

Proliferation of NHOst cells cultured with the apatites was estimated by Tetracolor One assay (Seikagaku Co., Ltd. Tokyo, Japan), which incorporates an oxidation reduction indicator based on detection of metabolic activity. After 7-days incubation, 2%-TetraColor One/αMEM solution was added to each well, followed by 2h incubation. The absorbance of the supernatant at 450nm was estimated using μQuant spectrophotometer (Bio-tek Instrument, Inc., Winooski, VT). After estimating the proliferation, the cells were washed by phosphate–buffered saline (PBS(-)), followed by addition of 1ml of 0.1M glycine buffer (pH=10.5) containing 10mM $MgCl_2$, 0.1mM $ZnCl_2$ and 4mM p-nitrophenylphosphate sodium salt. After incubating at room temperature for 5min, the absorbance at 405 nm was detected using the μQuant spectrophotometer to evaluated alkaline phosphatase (ALP) activity of the test cells.

Results and Discussion

XRD patterns of NbHAps prepared by wet chemical process are shown in Fig.1(a). Irrespective of Nb/(Nb+P) molar ratio in starting solution, the precipitates were identified as monolithic HAp.

Table1. The ionic content of starting solution and the composition of the obtained precipitates.

Samples	Ionic content of Starting Solution*,			Theoretical Ca/(Nb+P)**	Nb/(Nb+P)**		Color of Precipitates
	Ca	PO_4	Nb		Theoretical	Measured***	
HAp	60.0	36.0	0.0	1.67	0.0000	-	White
NbHAp-I	60.0	35.4	0.6	1.67	0.0167	0.015	Pale yellow
NbHAp-II	60.0	30.0	6.0	1.67	0.1667	0.082	Buff yellow

*mmol, **Molar ratio, ***The precipitates were dissolved with HCl and the ionic concentration of HCl solutions were measured by ICP.